JOC Article

Design Criteria for Ionic Liquid Crystalline Phases of Phosphonium Salts with Three Equivalent Long *n*-Alkyl Chains

Kefeng Ma,[†] Kwang-Ming Lee,[‡] Liliya Minkova,[§] and Richard G. Weiss*,[†]

Department of Chemistry, Georgetown University, Washington, DC 20057-1227

weissr@georgetown.edu

Received November 26, 2008

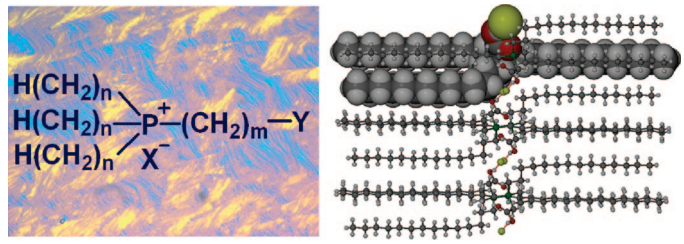

The factors influencing the formation, organizations, and temperature ranges of the smectic phases of a structurally diverse family of phosphonium salts have been examined. The salts consist of one short group and three long *n*-alkyl chains attached to a positively charged phosphorus atom and either a free or covalently attached counterion, the latter resulting in zwitterionic salts. Of the 61 salts investigated, of which 37 have not been synthesized previously, most pack in lamellae within their solid phases. Single-crystal X-ray structures of two of amidomethyl-tri-*n*-tetradecylphosphonium bromide (**1P14CONH$_2$Br**) and carboxymethyl-tri-*n*-tetradecylphosphonium bromide (**1P14-CO$_2$HBr**) have been solved. In each, the constituent molecules are packed in stacks of bilayers in which the directors of molecules on opposite sides of the ionic planes (where the phosphonium cationic centers and anions are located) that separate the layers are antiparallel. In each molecule, two of the long *n*-alkyl chains are paired while the third is antiparallel to the other two and paired with an *n*-alkyl chain of a molecule in a neighboring bilayer. The tri-*n*-alkylmethylphosphonium salts (**1P*n*X**) with small anions X (where $n = 6-18$ is the number of carbon atoms in the three long chain and 1 is the methyl group) do not form liquid-crystalline phases as a consequence of strong alternating intra- and intermolecular P^+-X^- interactions within the ionic planes that separate the bilayers of long chains. Thermotropic and enantiotropic liquid-crystalline phase formation of **1P*n*X** salts is favored by larger anions and longer *n*-alkyl chains, which reduce order within ionic planes while promoting order within the lipophilic layers. We conjecture that covalent attachment of a hydroxymethylene, carboxy, or amido functional group Y to the α-methyl group of a **1P*n*X** salt (resulting in ***m*P*n*YX** salts, where *m* is the number of methylene units separating the phosphorus atom from the Y group on the short chain) moves the anion X farther from the P^+ ion as a result of intramolecular $X^-\cdots H(Y)$ H-bonding interactions and, therefore, substantially weakens intramolecular P^+-X^- ionic interactions within the ionic planes. In contrast to the trends mentioned for the **1P*n*X** salts, liquid-crystalline phases of ***m*P*n*YX** are found more frequently when *n* is shorter and X is smaller. The observation that the liquid-crystalline phases of ***m*P*n*YX** salts have lower clearing and onset temperatures than the corresponding **1P*n*X** may be attributed to the greater freedom of motion at and near the ionic planes of the former as a result of their more dispersed ionic interactions. Overall, a detailed study of the dependence of phase type and phase transition temperatures on several key structural factors of phosphonium salts has been made. The correlations found provide insights into how new mesmorphic phosphonium salts can be designed and exploited for a wide range of potential applications.

Introduction

Ionic liquids (ILs), defined commonly to be molten salts with melting points below 100 °C,[1] are a subject of continuing interest because their properties can be tuned for many applications.[2] In addition to being "green" solvents,[3] ILs have been used for

[†] Georgetown University.

[‡] Current address: Department of Chemistry, National Kaoshsiung Normal University, 62 Shen-Chung Road, Kaohsiung 824, Taiwan, ROC.

[§] Current address: Bulgarian Academy of Sciences, Institute of Polymers, BU-1113 Sofia, Bulgaria.

(1) (a) Abedin, S. Z. E.; Endres, F. *Acc. Chem. Res.* **2007**, *40*, 1106–1113. (b) Rogers, R. D.; Voth, G. A. *Acc. Chem. Res.* **2007**, *40*, 1077–1078. (c) *Ionic Liquids III: Fundamentals, Progress, Challenges, and Opportunities*; Rogers, R. D., Seddon, K. R., Eds.; ACS Symposium Series 901−902; American Chemical Society: Washington, DC, 2005.

(2) Smiglak, M.; Metlen, A.; Rogers, R. D. *Acc. Chem. Res.* **2007**, *40*, 1182–1192.

10.1021/jo802605k CCC: $40.75
Published on Web 02/11/2009

a myriad of applications in diverse synthetic reactions,[4,5] separations and extractions,[6] and electrochemical,[7] nanotechnological,[8] biotechnological,[9] and engineering[10] processes. Appropriately designed ionic liquids may also be liquid crystalline over temperature ranges that are smaller than those of the liquid phase.[11] In those cases, their anisotropic orientations are driven by electrostatic interactions and microsegregation between ionic and lipophilic regions.[12] The physical and chemical properties of ionic liquid crystals (ILCs) can differ significantly from those of uncharged liquid crystals (LCs).[12a,13]

CHART 1. Molecular Structures of Phosphonium Salts (*m*P*n*YX) and Zwitterions (*m*P*n*Y) Investigated

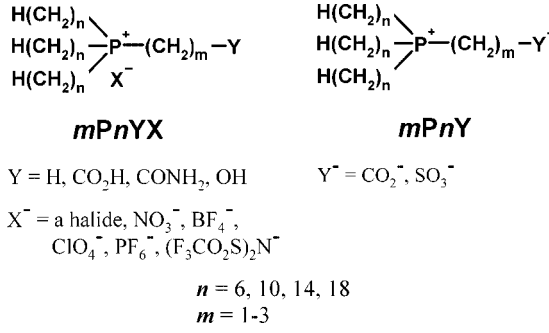

Previously, we have characterized the phase properties of a large number of phosphonium salts, $[H(CH_2)_n]_3P^+[(CH_2)_mY]\ X^-$ (***m*PnX**, where $n = 10$, 14, 18, $m = 0-5$ when Y = H and X^- is a halide, NO_3^-, ClO_4^-, BF_4^-, PF_6^-, etc.),[14] **1P18BzBr** (Bz = $C_6H_5CH_2$),[15] and recently ***m*PnYX** where $m =$ and Y = OH (**2P*n*OHX** with X = Cl or Br) (Chart 1).[16] Many of these salts form enantiotropic, bilayer smectic A liquid-crystalline phases (SmA_2),[17] and some single-crystal data for their analogues (N.B., benzyl-tri-*n*-octadecylammonium bromide[15] and phosphonium salts with 4 equivalent, long *n*-alkyl chains[18]) are available. Although **1P14Br** exhibits a narrow range mesomorphic phase ($T_{K-SmA_2} = 103.6-104.7$ °C, $T_{SmA_2-I} = 113.2-114.0$ °C; K = solid and I = isotropic) when neat, amphotropic and lyotropic SmA_2 phases can be induced in **1P*n*X** salts (with $n = 10$ or 14 and X = Cl or Br) upon addition of one or more molar equivalents of water or an alcohol. The mesophases have low (subambient in some cases) onset temperatures and broad mesomorphic temperature ranges.[19] The initiation of liquid crystallinity derives from intermolecular interactions between the hydroxyl groups of water or an alcohol molecule and the charged centers of the **1P*n*X** salts that attenuate the P^+-X^- electrostatic interactions within bilayers.

The structural simplicity, saturated nature, ease of synthesis, wide structural diversity, transparency in the visible and near UV regions, and higher stability toward thermal and chemical degradation compared with that of their homologous ammonium salts[20] make these salts promising for a wide variety of applications. For example, several ***m*P18X** salts have been employed as templating agents to form porous, nanostructured

(3) (a) Plechkova, N. V.; Seddon, K. R. In *Methods and Reagents for Green Chemistry*; Tundo, P., Perosa, A., Zecchini, F., Eds.; Wiley: Hoboken, NJ, 2007; pp 103−130. (b) *Ionic Liquids as Green Solvents, Progress and Prospects*; Rogers, R. D., Seddon, K. R., Eds.; ACS Symposium Series 856; American Chemical Society: Washington, DC, 2003. (c) Rogers, R. D.; Seddon, K. R.; Volkov, S. *Green Industrial Applications of Ionic Liquids*; Kluwer Academic Publishers: Norwell, MA, 2003. (d) *Ionic Liquids: Industrial Applications for Green Chemistry*; Rogers, R. D.; Seddon, K. R., Eds.; ACS Symposium Series 818; American Chemical Society: Washington, DC, 2002. (e) Earle, M. J.; Seddon, K. R. *Pure Appl. Chem.* **2000**, *72*, 1391–1398.

(4) (a) Haumann, M.; Riisager, A. *Chem. Rev.* **2008**, *108*, 1474–1497. (b) Parvulescu, V. I.; Hardacre, C. *Chem. Rev.* **2007**, *107*, 2615–1665. (c) Dupont, J.; de Souza, R. F.; Suarez, P. A. Z. *Chem. Rev.* **2002**, *102*, 3667–3692.

(5) (a) Martins, M. A. P.; Frizzo, C. P.; Moreira, D. N.; Zanatta, N.; Bonacorso, H. G. *Chem. Rev.* **2008**, *108*, 2015–2050. (b) Miao, W.; Chan, T. H. *Acc. Chem. Res.* **2006**, *39*, 897–908. (c) *Ionic Liquids in Organic Synthesis*; Malhotra, S. V., Ed.; ACS Symposium Series 950; American Chemical Society: Washington, DC, 2007. (d) Wasserscheid, P.; Welton, T. *Ionic Liquids in Synthesis*; Wiley-VCH: Weinheim, 2003. (e) Welton, T. *Chem. Rev.* **1999**, *99*, 2071–2083.

(6) (a) Han, X.; Armstrong, D. W. *Acc. Chem. Res.* **2007**, *40*, 1079–1086. (b) Anjan, S. T. *Chem. Eng. Prog.* **2006**, *102*, 30–39. (c) Zhao, H.; Xiao, S.; Ma, P. *J. Chem. Technol. Biotechnol.* **2005**, *80*, 1089–1096. (d) Visser, A. E.; Swatloski, R. P.; Reichert, W. M.; Mayton, R.; Sheff, S.; Wierzbicki, A.; Davis, J. H.; Rogers, R. D. *Environ. Sci. Technol.* **2002**, *36*, 2523–2529. (e) Huddleston, J. G.; Rogers, R. D. *Chem. Commun.* **1998**, *16*, 1765–1766.

(7) (a) Hapiot, P.; Lagrost, C. *Chem. Rev.* **2008**, *108*, 2238–2264. (b) MacFarlane, D. R.; Forsyth, M.; Howlett, P. C.; Pringle, J. M.; Sun, J.; Annat, G.; Neil, W.; Izgorodina, E. I. *Acc. Chem. Res.* **2007**, *40*, 1165–1173. (c) *Electrochemical Aspects of Ionic Liquids*; Ohna, H., Ed.; Wiley: Hoboken, NJ, 2005.

(8) (a) Ichikawa, T.; Yoshio, M.; Hamasaki, A.; Mukai, T.; Ohno, H.; Kato, T. *J. Am. Chem. Soc.* **2007**, *129*, 10662–10663. (b) Biswas, K.; Rao, C. N. R. *Chem.−Eur. J.* **2007**, *13*, 6123–6129. (c) Wang, Y.; Yang, H. *J. Am. Chem. Soc.* **2005**, *127*, 5316–5317. (d) Zhu, Y.; Wang, W.; Qi, R.; Hu, X. *Angew. Chem., Int. Ed.* **2004**, *43*, 1410–1414.

(9) Rantwijk, F. V.; Sheldon, R. A. *Chem. Rev.* **2007**, *107*, 2757–2785.

(10) (a) Greaves, T. L.; Drummond, C. J. *Chem. Rev.* **2008**, *108*, 206–2037. (b) Schneider, S.; Hawkins, T.; Rosander, M.; Vaghjiani, G.; Chambreau, S.; Drake, G. *Energy Fuels* **2008**, *22*, 2871–2872. (c) Zhao, H. *Chem. Eng. Commun.* **2006**, *193*, 1660–1677.

(11) (a) Matsunaga, Y.; Tsujimura, T. *Mol. Cryst. Liq. Cryst.* **1991**, *200*, 103–108. (b) Boy, P.; Cornbellas, C.; Mathey, G.; Palacin, S.; Persoons, A.; Thiébault, A.; Verbiest, T. *Adv. Mater.* **1994**, *6*, 580–583. (c) Tabrizian, M.; Soldera, A.; Couturier, M.; Bazuin, G. C. *Liq. Cryst.* **1995**, *18*, 475–482. (d) Kanazawa, A.; Tsutsumi, O.; Ikeda, T.; Nagase, Y. *J. Am. Chem. Soc.* **1997**, *119*, 7670–7675. (e) Gordon, C. M.; Holbrey, J. D.; Kennedy, A. R.; Seddon, K. R. *J. Mater. Chem.* **1998**, *8*, 2627–2636. (f) Holbrey, J. D.; Seddon, K. R. *J. Chem. Soc., Dalton Trans.* **1999**, 2133–2139. (g) Ohta, Sugiyama, T.; Nogami, T. *J. Mater. Chem.* **2000**, *10*, 613–616. (h) Bradley, A. E.; Hardacre, C.; Holbrey, J. D.; Johnston, S.; McMath, S. E. J.; Nieuwenhuyzen, M. *Chem. Mater.* **2002**, *14*, 629–635. (i) De Roche, J.; Gordon, C. M.; Imrie, C. T.; Ingram, M. D.; Kennedy, A. R.; Lo Celso, F. L.; Triolo, A. *Chem. Mater.* **2003**, *15*, 3089–3097. (j) Tsiourvas, D.; Paleos, C. M.; Skoulios, A. *Chem.−Eur. J.* **2003**, *9*, 5250–5258. (k) Mukai, T.; Yoshio, M.; Kato, T.; Hiroyuki, O. *Chem. Lett.* **2004**, *33*, 1630–1631. (l) Suisse, J.-M.; Bellemin-Laponnaz, S.; Douce, L.; Maisse-Francois, A.; Welter, R. *Tetrahedron Lett.* **2005**, *46*, 4303–4305. (m) Godinho, M. H.; Cruz, C.; Teixeira, P. I. C.; Ferreira, A. J.; Costa, C.; Kulkarni, P. S.; Afonso, C. A. M. *Liq. Cryst.* **2008**, *35*, 103–107. (n) Greaves, T. L.; Drummond, C. J. *Chem. Rev.* **2008**, *108*, 206–237. (o) Greaves, T. L.; Drummond, C. J. *Chem. Soc. Rev.* **2008**, *37*, 1709–1726.

(12) (a) Binnemans, K. *Chem. Rev.* **2005**, *105*, 4148–4204. (b) Samanta, A. *J. Phys. Chem. B* **2006**, *110*, 13704–13716. (c) Yang, J.; Zhang, Q.; Zhu, L.; Zhang, S.; Li, J.; Zhang, X.; Deng, Y. *Chem. Mater.* **2007**, *19*, 2544–2550. (d) Kouwer, P. H. J.; Swager, T. M. *J. Am. Chem. Soc.* **2007**, *129*, 14042–14052. (e) Trilla, M.; Pleixats, R.; Parella, T.; Blanc, C.; Dieudonné, P.; Guari, Y.; Man, M. W. C. *Langmuir* **2008**, *24*, 259–265. (f) Yazaki, S.; Funahashi, M.; Kato, T. *J. Am. Chem. Soc.* **2008**, *130*, 13206–13207.

(13) (a) Faul, C. F. J.; Antonietti, M. *Adv. Mater.* **2003**, *15*, 673–683. (b) Kato, T. *Science* **2002**, *295*, 2414–2418.

(14) (a) Abdallah, D. J.; Robertson, A.; Hsu, H.; Weiss, R. G. *J. Am. Chem. Soc.* **2000**, *122*, 3053–3062. (b) Chen, H.; Kwait, D. C.; Gönen, Z. S.; Weslowski, B. T.; Abdallah, D. J.; Weiss, R. G. *Chem. Mater.* **2002**, *14*, 4063–4072. (c) Nagana Gowda, G. A.; Chen, H.; Khetrapal, C. L.; Weiss, R. G. *Chem. Mater.* **2004**, *16*, 2101–2106. (d) Nagana Gowda, G. A.; Khetrapal, C. L.; Lu, L.; Wauters, H. C.; Abdallah, D. J.; Weiss, R. G. *Proc. Ind. Nat. Sci. Acad. U.S.A.* **2004**, *70A*, 627–634.

(15) Abdallah, D. J.; Lu, L.; Cocker, M. T.; Bachman, R. E.; Weiss, R. G. *Liq. Cryst.* **2000**, *27*, 831–837.

(16) Ma, K.; Somashekhar, B. S.; Nagana Gowda, G. A.; Khetrapal, C. L.; Weiss, R. G. *Langmuir* **2008**, *24*, 2746–2758.

(17) A bilayer smectic A phase is denoted as SmA_2. Demus, D.; Goodby, J.; Gray, G. W.; Spiess, H.-W.; Vill, V. *Handbook of Liquid Crystals, High Molecular Weight Liquid Crystals*; Wiley-VCH: New York, 1998; Vol. 3, p 312.

(18) Abdallah, D. J.; Bachman, R. E.; Perlstein, J.; Weiss, R. G. *J. Phys. Chem. B* **1999**, *103*, 9269–9278.

(19) Ma, K.; Shahkhatuni, A. A.; Somashekhar, B. S.; Nagana Gowder, G. A.; Tong, Y.; Khetrapal, C. L.; Weiss, R. G. *Langmuir* **2008**, *24*, 9843–9854.

(20) (a) Malliaris, A.; Christias, C.; Margomenou-Leonidopoulou, G.; Paleos, C. M. *Mol. Cryst. Liq. Cryst.* **1982**, *82*, 161–166. (b) Iwamoto, K.; Ohnuki, Y.; Sawada, K.; Seno, M. *Mol. Cryst. Liq. Cryst.* **1981**, *73*, 95–103. (c) Bradaric, C. J.; Downard, A.; Kennedy, C.; Robertson, A. J.; Zhou, Y. *Green Chem.* **2003**, *5*, 143–152. (d) Kim, Y. J.; Varma, R. S. *J. Org. Chem.* **2005**, *70*, 7882–7891.

silica and titania objects.[21] The ionic liquid methyl-tri-*n*-decylphosphonium tribromide (**1P10Br$_3$**) has been exploited as a recyclable and "green" brominating agent that demonstrates stereoselectivities different from those of many other reagents.[22] Ionic liquids of trihexyltetradecylphosphonium salts have been used as media in palladium-catalyzed carbonylation reactions.[23] Liquid-crystallinity of phosphonium salts may impart unique stereo- and regiocontrols over solute reactions that isotropic salts do not.[24] Because they are much easier to align in magnetic fields and their order parameters are generally much lower ($\sim 10^{-2}$)[14d,16,19,25] than those of other thermotropic smectic phases that lack a higher temperature nematic phase, SmA_2 phases of phosphonium salts also hold promise as nonaqueous, nonpolymeric hosts in NMR studies to determine the molecular geometries and orientations of solute molecules.[26]

Thus, it is important to ascertain the structural factors that lead to liquid crystallinity in phosphonium salts so that reliable design criteria for specific uses are available. Here, we explore those criteria. They include variations of the short chain length or terminal functionality (*m* or Y, respectively), the length of the long chains (*n*), and the nature of the anions (X) on phase properties. Among the new materials synthesized and characterized are phosphonium salts (***m*P*n*YX**), with a hydroxymethylene, carboxy, or amido functional group Y covalently attached to the α-methyl group of a **1P*n*X** salt, and zwitterions (***m*P*n*CO$_2$** and **3P*n*SO$_3$**), which consist of a carboxylate or sulfonate anion connected covalently to the end of the shortest chain (Chart 1). The analyses rely heavily upon the single-crystal data for **1P14CONH$_2$Br** and **1P14CO$_2$HBr** and their relationship to the packing of the other phosphonium salts (as indicated by comparisons among powder X-ray diffractions of other salts). A comparison of structure and phase properties among the ***m*P*n*YX** and **1P*n*X** and the trends in the phase properties detected among the different variables leads to a comprehensive hypothesis for what is needed structurally to stabilize a liquid-crystal phase.

Results and Discussions

Thermogravimetric Analyses (TGA) and Infrared Spectroscopy (IR). Decarboxylation of **1P*n*CO$_2$HBr** commences near 130 °C. In the temperature range of ca. 130−165 °C, the TGA data show 7.4%, 5.8%, and 4.7% weight losses from **1P*n*CO$_2$HBr** with $n = 10$, 14, and 18, respectively. These are the expected weight losses for removal of carbon dioxide (Table S1 of Supporting Information), and decarboxylation of salts with a β-carboxylate is known[27] (Figure S1 of Supporting Information). The IR spectra of the materials remaining after the **1P*n*CO$_2$HBr** were heated to 165 °C and then cooled to room temperature lack the strong 1723 cm^{-1} peak from C═O stretching and the broad 2300−3300 cm^{-1} peak from O−H stretching that were present in the unheated materials (Figure 1). The IR spectra of the corresponding (dehydrohalogenated) zwitterions, **1P*n*CO$_2$**, have a low frequency C═O stretch at 1625 cm^{-1} and no discernible O−H absorptions, as expected (Figure 1). The thermal stabilities of the **1P*n*CO$_2$** are low because of their propensity to lose CO_2, as well (Table S1 of Supporting Information). **2P*n*CO$_2$**, where the carboxyl group is moved to the γ position from the P^+ center (i.e., insertion of an additional methylene between the carboxy and P^+ groups of **1P*n*CO$_2$**), are much more stable thermally; they suffer decarboxylation at ca. 185 °C. The other phosphonium salts and zwitterions investigated here are stable thermally to ≥200 °C.

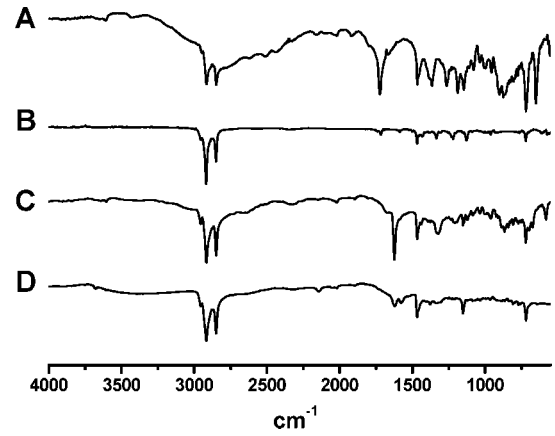

FIGURE 1. Room temperature IR spectra of (A) **1P14CO$_2$HBr** and (B) **1P14CO$_2$HBr** after being heated to 165 °C for 5 min and (C) **1P14CO$_2$** and (D) **1P14CO$_2$** after being heated to 80 °C for 5 min.

Single-Crystal X-ray Structure Analyses of 1P14CO$_2$HBr and 1P14CONH$_2$Br.[28] Because some of the conformational and packing features of the solid and liquid-crystalline phases may be shared, we attempted to grow single crystals for X-ray analyses of the salts investigated here. It was possible to obtain suitable crystals of **1P14CO$_2$HBr** and **1P14CONH$_2$Br** from solutions of ethyl acetate and acetonitrile, respectively. Both phosphonium cations adopt an "h"-shape conformation at the molecular level, and three *gauche* bends with two *transoid* bends in between allow two of three *n*-tetradecyl chains to be paired in parallel at one side of the phosphorus ion for a ca. 7.2 Å space between them (Figures S2 and S3 of Supporting Information), as in phosphonium salts with four long *n*-alkyl chains[18] and benzyltrioctadecylammonium bromide.[15] The third, nonpaired *n*-tetradecyl chain is projected in the opposite direction with an all-*transoid* conformation along the axis parallel to the paired chains. The shortest group attached to phosphorus is pointed in a direction nearly orthogonal to the approximate plane defined by three long *n*-tetradecyl chains. Some selected bond lengths and angles from the single-crystal structures of **1P14CONH$_2$Br** and **1P14CO$_2$HBr** are listed in Table S2 of Supporting Information.

(21) Huang, X.; Weiss, R. G. *Langmuir* **2006**, *22*, 8542–8552.
(22) Ma, K.; Li, S.; Weiss, R. G. *Org. Lett.* **2008**, *10*, 4155–4158.
(23) (a) Cao, H.; McNamee, L.; Alper, H. *Org. Lett.* **2008**, *10*, 5281–5284. (b) Yang, Q.; Robertson, A.; Alper, H. *Org. Lett.* **2008**, *10*, 5079–5082. (c) Cao, H.; McNamee, L.; Alper, H. *J. Org. Chem.* **2008**, *73*, 3530–3534. (d) Mcnulty, J.; Nair, J. J.; Robertson, A. *Org. Lett.* **2007**, *9*, 4575–4578.
(24) (a) Lemieux, R. P. *Acc. Chem. Res.* **2001**, *34*, 845–853. (b) Reichardt, C. *Solvent and Solvent Effects in Organic Chemistry*, 3rd ed.; Wiley-VCH: Weinheim, 2003. (c) Ichimura, K. *Chem. Rev.* **2000**, *100*, 1847–1873. (d) Kansui, H.; Hiraoka, S.; Kunieda, T. *J. Am. Chem. Soc.* **1996**, *118*, 5346–5352. (e) Weiss, R. G. In *Photochemistry in Organized and Constrained Media*; Ramamurthy, V., Eds.; VCH Publishers: New York, 1991; Chapter 14. (f) Weiss, R. G. *Tetrahedron* **1988**, *44*, 3413–3475. (g) Weiss, R. G. *Tetrahedron* **1988**, *44*, 3413–3475.
(25) Lu, L.; Sharma, N.; Nagana Gowda, G. A.; Khetrapal, C. L.; Weiss, R. G. *Liq. Cryst.* **1997**, *22*, 23–28.
(26) (a) Diehl, P.; Khetrapal, C. L. In *NMR Basic Principles and Progress*; Diehl, P., Fluck, E., Kosfeld, R., Eds.; Springer-Verlag: New York, 1969; Vol. 1. (b) Meiboom, S.; Snyder, L. C. *Acc. Chem. Res.* **1971**, *4*, 81–87. (c) Jacobsen, J. P.; Schaumburg, K. *J. Magn. Reson.* **1977**, *28*, 191–201. (d) Tjandra, N.; Bax, A. *Science* **1997**, *278*, 1111–1114. (e) Vivekanandan, S.; Joy, A.; Suryaprakash, N. *J. Mol. Struct.* **2004**, *694*, 241–247. (f) Bax, A.; Grishaev, A. *Curr. Opin. Struct. Biol.* **2005**, *15*, 563–570.
(27) Chopard, P. A. *J. Org. Chem.* **1966**, *31*, 107–111.
(28) CCDC 710295 and 710296 contain supplementary crystallographic data for **1P14CO$_2$HBr** and **1P14CONH$_2$Br**. This information can be obtained online (http://www.ccdc.cam.ac.uk/) free of charge (or from the Cambridge Crystallographic Data Centre, 12 Union Road, Cambridge CB2 1EZ, U.K., fax (+44) 1223-336-033, or deposit@ccdc.cam.ac.uk).

TABLE 1. Crystal Data for 1P14CONH$_2$Br and 1P14CO$_2$HBr

compound	**1P14CONH$_2$Br**	**1P14CO$_2$HBr**
chemical formula	$C_{44}H_{91}BrNOP$	$C_{44}H_{90}BrO_2P$
formula weight	761.06	762.04
temperature/°C	−100(2)	−100(2)
crystal size (mm)	0.60 × 0.50 × 0.14	0.65 × 0.45 × 0.10
crystal system	monoclinic	monoclinic
space group	*P*2(1)/*c*	*P*2(1)/*c*
space group number	14	14
a (Å)	21.568(3)	22.004(12)
b (Å)	14.199(2)	14.111(8)
c (Å)	15.455(2)	15.110(8)
α (deg)	90	90
β (deg)	96.566(3)	100.015(10)
γ (deg)	90	90
V (Å^3)	4701.9(13)	4620(4)
Z	4	4
F(000)	1680	1680
reflections collected	50811	21607
independent reflections	11371	8941
R^a	0.0414	0.0458
$R_w{}^b$	0.0825	0.0732
variables	433	433

^{a} $R = \Sigma||F_o - F_c||\Sigma F_o$. ^{b} $R_w(F_o)^2 = [\Sigma_w(F_o^2 - F_c^2)^2/\Sigma_w F_o^4]^{1/2}$.

The molecules are arrayed in parallel but with their long molecular axes alternating in opposite orientations for a monoclinic bilayer crystal structure (Table 1) in which the phosphorus cations and bromide anions occupy alternating locations within a plane (Figure 2A and Figure S4 of Supporting Information). The orientations between two adjacent ionic layerings along the *b* axis are also reversed. The long alkyl chains are completely interdigitated between molecular bilayers, and the long molecular axis is perpendicular to the ionic plane. Two molecules define the thickness of this bilayered lamellar structure, which is the length of the *a*-axis in a unit cell, 21.6 and 22.0 Å, respectively, for **1P14CONH$_2$Br** and **1P14CO$_2$HBr**. These two functionalized phosphonium bromides display a totally different packing arrangement from the salts with four long *n*-alkyl chains for a noninterdigitated lamellar structure[18] and benzyl-trioctadecylammonium bromide for an alternating interdigitated and noninterdigitated lamellar structure.[15]

The bromide ions are pushed forward in the extended position of the short headgroup by its H-bonding with the hydrogen of the carboxyamide or carboxyl group, and the Br$^-$ anion of **1P14CONH$_2$Br** is further away from the P$^+$ ion (6.98 Å) than that of **1P14CO$_2$HBr** (6.70 Å); the carboxyamide group occupies a larger cross-sectional area allocated to each **1P14CONH$_2$Br** molecule as projected onto an ionic layer plane than the carboxyl group does in **1P14CONH$_2$Br**. A slightly longer distance between P$^+$ and Br− (and, perhaps, weaker electrostatic interactions) from two adjacent oppositely oriented **1P14CONH$_2$Br** molecules (4.04 Å) than that from the **1P14CO$_2$HBr** molecules (4.02 Å) is found along the ionic layering *b* axis. The length of the *b*-axis along the ionic layering is slightly longer in **1P14CONH$_2$Br** (14.2 Å) than in **1P14CO$_2$HBr** (14.1 Å). As a result and consistent with the shorter spacing between the outmost hydrogen of the nonpaired alkyl chain and the P$^+$ ion from the adjacent layer along the *a* axis of **1P14CONH$_2$Br** (3.20 Å) compared with that of **1P14CO$_2$HBr** (3.63 Å), there is slightly more interdigitation of long chains between bilayers of **1P14CONH$_2$Br** than between those of **1P14CO$_2$HBr**. A network of hydrogen-bonding interactions summarized in Table S3 of Supporting Information is suggested by interatomic distances between the center of the bromide anion or the carbonyl oxygen atom and several hydrogens from neighboring molecules that are much shorter than the sum of the van der Waals radii of hydrogen and bromide (3.16 Å) or hydrogen and oxygen (2.72 Å)[29] (Figure 2B and C).

Our previously proposed molecular structure for the **1P*n*X** salts, which is based on the single-crystal structure of benzyltrioctadecylammonium bromide, is different from that of the functionalized **1P*n*YX** salts here, but both packing arrangements adopt similar bilayer stacking structures in which three long alkyl chains are more or less interdigitated. The peaks from powder X-ray diffractograms of the **1P10X** and **2P*n*OHX** salts (n =10, 14; X = Cl, Br) could be indexed to monoclinic crystal systems and, probably, in the *P*2(1)/*c* space group as well. The degree to which the packing arrangements of the **1P*n*X** and the ***m*P*n*YX** salts differ, especially in their liquid-crystalline phases, is unknown because the powder data do not provide sufficient details. However, the generally greater degree of interdigitation between bilayers in the crystal phase for the functionalized **1P*n*YX** salts may be a consequence of the intermolecular hydrogen bonding interactions involving the carboxyamide and carboxyl groups.

The single-crystal structures of **1P14CONH$_2$Br** and **1P14-CO$_2$HBr** indicate that intramolecular X$^-$···H(Y) H-bonding interactions of ***m*P*n*YX** salts are more important than P$^+$−X$^-$ ionic interactions; the ionic layers of these salts consist of alternating weak intramolecular X$^-$···H(Y) and strong intermolecular P$^+$−X$^-$ ionic interactions. Extrapolating from the single-crystal structure of 4-methyl-4-*p*-nitrobenzyl-4phosphoniatetracyclo[3.3.0.0^{2,8}.0^{3,6}]octane bromide,[30] the small α-methyl groups of **1P*n*X** salts should allow relatively strong intramolecular P$^+$−X$^-$ ionic interactions as well as weak X$^-$···H(α-CH$_3$) H-bonding interactions, and those interactions result in better-defined lamellar packing structures than in the corresponding ***m*P*n*YX** salts.

Optical Textures and Phase Transition Temperatures from Polarized Optical Microscopy (POM). When cooled from the isotropic phase, liquid-crystalline ***m*P*n*YX** samples showed no optical birefringence: they were homeotropically oriented, and the molecular directors are orthogonal to the lamellar plane (as confirmed by X-ray diffraction data (vide infra)). However, oily streak textures were induced in the liquid-crystalline phases by lateral shearing (Figure 3) or when by melting the solid samples. Like the **1P*n*X** salts,[14a,b] the mesomorphic ***m*P*n*YX** salts form interdigitated smectic A (SmA$_2$) phases that are enantiotropic (i.e., they can be formed by melting the solids or by cooling the isotropic liquid phases). Melting temperatures (T_M) from solid (K) → SmA$_2$ transitions and clearing temperatures (T_C) from either SmA$_2$ → isotropic (I) or K → I transitions were determined by optical microscopy by heating the samples (Figure 4 and Table S4 of Supporting Information).

Substitution of an H-atom by a hydroxymethylene, carboxy, or amido functional group Y at the α-methyl group of a **1P*n*X** increases the area each molecule projects onto its ionic layer plane and, thus, decreases the overall electrostatic interactions among the alternating P$^+$−X$^-$ ionic centers. On this basis, ***m*P*n*YX** molecules should have less compact lamellar structures

(29) Bondi, A. *J. Phys. Chem.* **1964**, *68*, 441–451.

(30) Mazhar-ul-Haque; Rashid, M.; Cremer, S. E. *J. Chem. Soc., Perkin Trans. 2* **1978**, 1115−1119. The distances of P$^+$−Br$^-$ and Br$^-$···H(α-CH$_3$) are 3.73 and 2.87 Å, respectively.

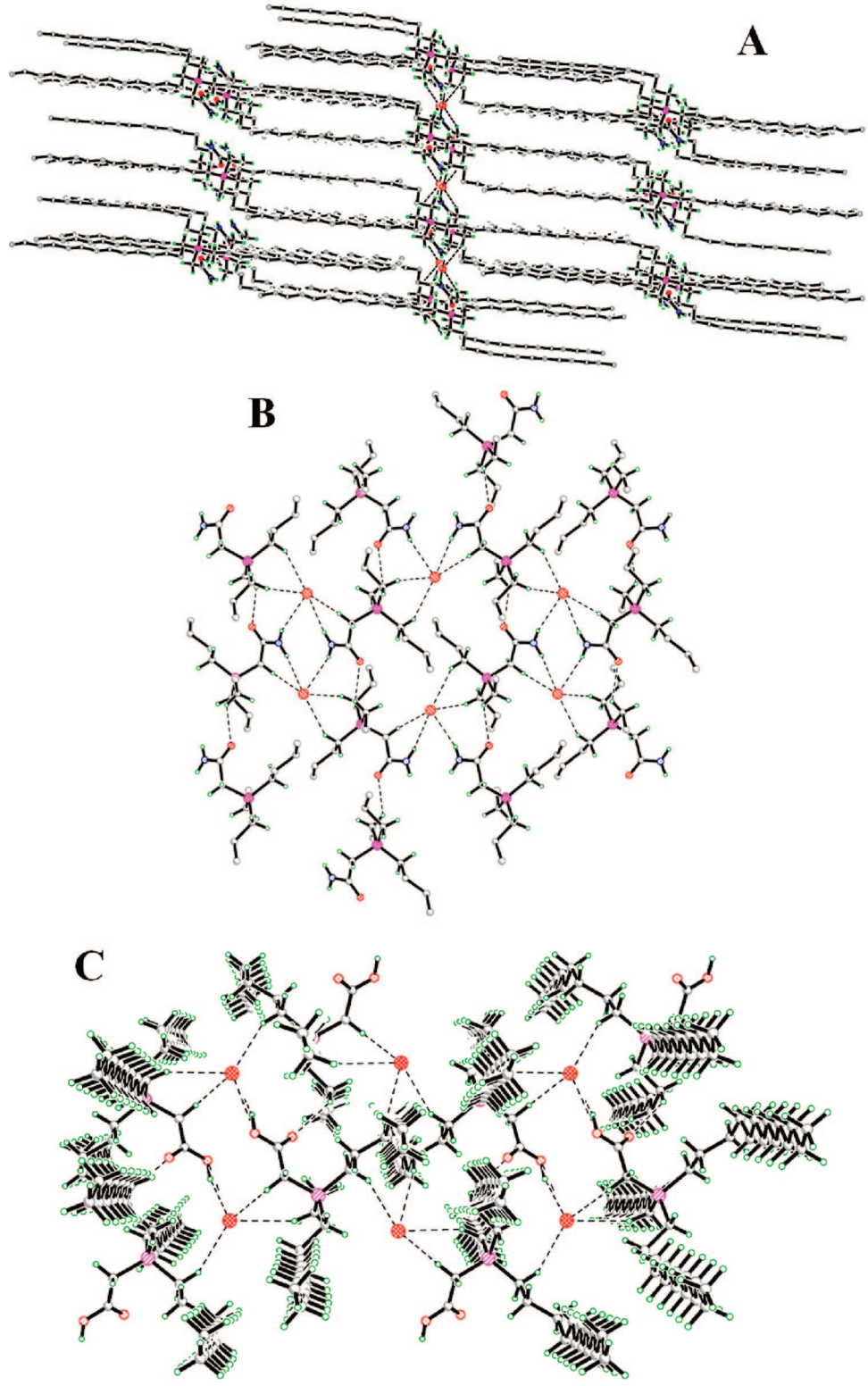

FIGURE 2. (A) Bilayer stacking structure of **1P14CONH$_2$Br** as viewed along *b* axis and the perspective view along the *a* axis of (B) **1P14CONH$_2$Br** and (C) **1P14CO$_2$HBr** showing the two-dimensional hydrogen-bonding network formed by intra- and intermolecular N−H···Br, O−H···Br, C−H···Br, and C−H···O hydrogen bonds.

than the corresponding **1P*n*X**. These factors allow the long alkyl chains and the ionic layering within lamellae to be more easily disturbed and clearing transition temperatures to be lowered (Figure 4). Consistent with this explanation, within a series of ***m*P*n*YX** in which only Y is changed, the clearing temperatures increase as the size of Y decreases: amido > carboxy > hydroxymethylene.

The clearing temperatures are affected by the size of the anions as well. Within a series of ***m*P*n*YX** in which only X is changed, T_C increases with increasing anionic radius up to X

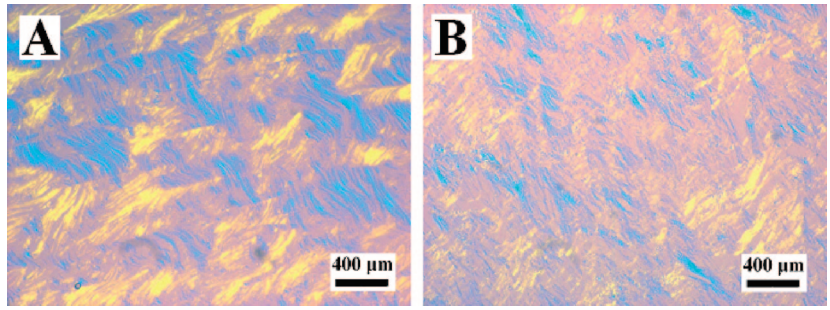

FIGURE 3. Polarized optical micrographs (POMs) of oily streak patterns from liquid-crystalline (A) **1P14CO$_2$HBr** at 82.0 °C and (B) **2P14OHBF$_4$** at 49.6 °C after being sheared between their cover glasses.

$= Cl^-$ ($r = 1.81$ Å; $r = 1.33$ Å (F^-) and 1.79 Å (NO_3^-)[31]) and decreases upon further size increases ($r = 1.96$ Å (Br^-), 2.20 Å (I^-), 2.20 Å (BF_4^-), 2.40 Å (ClO_4^-), and 2.95 Å (PF_6^-)[31]) (Figure 4). We conjecture that electrostatic interactions of the small sizes of the F^- and NO_3^- anions with the P^+ centers forces low polarity groups to fill some of the area/space within the ionic planes, and, thus, the network of intermolecular electrostatic interactions is attenuated; the smallest area that each phosphonium cation must occupy in its lamellar plane is determined by the compactness of the packing of its alkyl chains. That area can be no less than the sum of the van der Waals areas of the methylene groups on phosphorus. The larger anions can distribute themselves within the ionic layers without this constraint. When the total area of the molecules in which they reside exceeds the close-packing limit of the groups on phosphorus, the chains can adopt *gauche* bends to compensate.

On the basis of variations in T_C and T_{LC} in Figure 4A and B, the sensitivity of **1P*n*X** salts to structural changes near their ionic planes, largely from the nature of the anions X, is smaller than for the ***m*P*n*YX**. The sensitivity decreases also for one homologous series of **1P*n*X** or ***m*P*n*YX** as *n* increases from 10 to 18 (i.e., as the long alkyl chains dominate more the energy of packing); the stronger London dispersion interactions from longer alkyl chains lead to higher clearing and melting temperatures. In the other extreme, such as for **1P10Tf$_2$**, **1P10CONH$_2$Br**, and **2P10OHBF$_4$**, where the headgroup is large, the anion X is large, and the alkyl chains *n* are the shortest examined here, room-temperature ionic liquids are encountered.

Liquid crystals are favored among the ***m*P*n*X** salts with $m = 1$ (i.e., methyl as the fourth chain) when $n = 14$ or 18 and the anion X is large (Figure 4B). Liquid crystallinity and retention of lamellar packing are dependent on attractive energy contributions from electrostatic interactions to maintain the ionic layers and London dispersion forces that retard "melting" of the alkyl chains *n*. However, if either of these energies is too strong or too weak with respect to the other, melting will occur directly to the isotropic phase. In that regard, the smaller anions appear to form more well-defined ionic layers which cannot be disturbed sufficiently to allow the long *n*-alkyl chains to "melt" into a mesophase. At the same time, the more facile "melting" of the shorter *n* chains appears to allow disruption of the ionic layers without losing the lamellar order completely. The NO_3^- anion seems "abnormal" here because it is "loosely" situated between the P^+ ions in the ionic layers and fails to form as specific electrostatic interactions as discussed above (vide infra); thus, its ionic layers can adjust easily when the long *n*-alkyl chains melt.

The covalently attached functional group Y in the ***m*P*n*YX** salts with a small anion (i.e., X = Cl or Br) is assumed to reduce somewhat the strength of the ionic interactions of the P^+-X^- centers to values lower than those experienced by the corresponding **1P*n*X** salts. However, this does not result in a greater propensity of ***m*P*n*YX** salts to form liquid-crystalline phases with lower onset temperatures and broader temperature ranges. We conclude that the added disruption to the ionic layers and increased area each molecule projects onto the ionic planes are not offset by the London dispersion forces that maintain the lamellar packing about T_M. Shorter *n* chains (leading to lower T_M) and smaller X anions are needed to observe liquid crystallinity in the ***m*P*n*YX** salts.

None of the zwitterionic salts examined here, made by dehydrohalogenation of the ***m*P*n*YX** salts, exhibited liquid crystallinity. Instead, their clearing temperatures were higher than those of their precursor ***m*P*n*YX** salts. Also, the clearing temperature of **3P*n*SO$_3$** is slightly higher than that of **2P*n*CO$_2$** at the same *n*, but the T_C values decrease with increasing *n* (Figure 4C). Unlike the **1P*n*X** salts, addition of 1 equiv of water, an alcohol, or an *n*-alkane to the zwitterions does not induce liquid crystallinity (Table S5 of Supporting Information).

Differential Scanning Calorimetry (DSC). The high thermal stabilities of the phosphonium salts and zwitterions (not containing a carboxyl group) are indicated by their DSC thermograms and the TGA heating profiles discussed above. The differences between first and second heating thermograms, observed in some cases, result from the different melting characteristics of solid morphs obtained by solvent crystallization and melt cooling (Table 2); the morphs have been investigated by X-ray diffraction (vide infra). The entropies ($\Delta S = \Delta H/T_o$) of the thermodynamically reversible transitions, ΔS, were calculated using the averaged enthalpies (ΔH) in the second heating and cooling thermograms and the onset temperatures (T_o) calculated from the intersection of the peaks from these thermograms. Consistent with our assertion that the groups covalently attached to the methyl on phosphorus of the ***m*P*n*YX** reduce the ordering within the lamellae, the entropy changes during the $K \rightarrow SmA_2$ transitions (that include both a reduction of interdigitation between bilayers and an induction of liquid crystallinity; vide infra) of **2P14OHX** (X = Br or BF_4) and **1P14CO$_2$HBr** are smaller than the sum of those during the $K_1 \rightarrow K_2$ and $K_2 \rightarrow SmA_2$ transitions of the **1P14X** (Table 2 and Table S6 of Supporting Information). However, the $SmA_2 \rightarrow I$ entropy changes are very similar for the two sets of salts. Much

(31) (a) Marcus, Y. *Chem. Rev.* **1988**, *88*, 1475–1498. (b) Eliassaf, J.; Fuoss, R. M.; Lind, J. E., Jr. *J. Phys. Chem.* **1963**, *67*, 1941–1942. (c) Huheey, J. E. *Inorganic Chemistry*, 3rd ed.; Harper & Row: Cambridge, U.K., 1983.

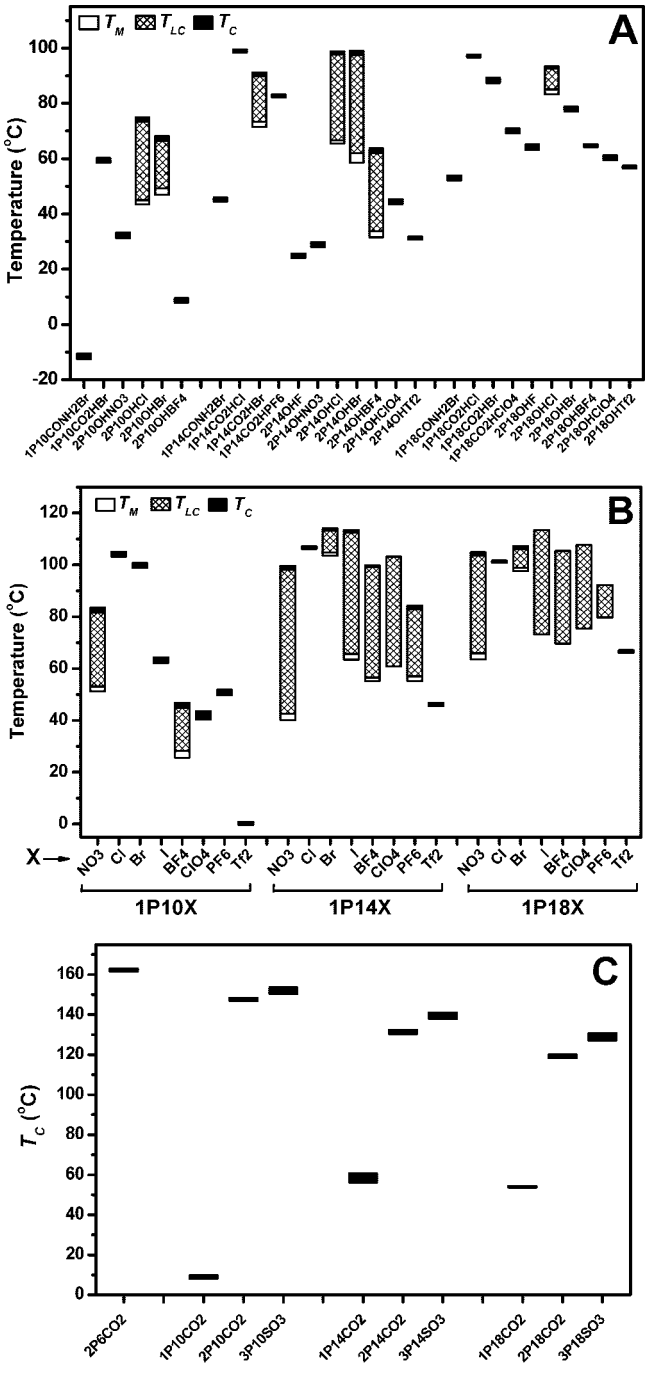

FIGURE 4. Phase transition temperatures of phosphonium salts: (A) **1P*n*CONH$_2$Br**, **1P*n*CO$_2$HX**, and **2P*n*OHX**, (B) **1P*n*X**, and (C) zwitterionic **1P*n*CO$_2$**, **2P*n*CO$_2$**, and **3P*n*SO$_3$** by optical microscopy on heating. The temperatures shown for the **1P*n*CO$_2$** are for decarboxylation and are obtained from DSC thermograms. The **1P*n*NO$_3$** and **1P14I** salts in (B) contain a trideutriomethyl group attached to phosphorus. Transition temperatures of **2P*n*OHX** and **1P*n*X** (X = Cl or Br) are from ref 16 and **1P*n*ClO$_4$** and **1P18X** (X = I, BF_4, or PF_6) are from ref 14a. $T_C = T_{K\rightarrow I}$ or $T_{SmA_2\rightarrow I}$; T_{LC} = smectic temperature range; $T_M = T_{K\rightarrow SmA_2}$.

more freedom of motion is gained when the ***m*P14YX** salts are melted. Similarly, the larger head groups of salts that have no mesophases result in smaller ΔS for K → I transitions of ***m*P*n*YX** salts than of **1PnX** salts.

As the length of long alkyl chains (n) increases, ΔS of the K → I transitions *increases* for the non-zwitterionic salts and *decreases* for the zwitterionic ones. In general, longer alkyl chains must suffer greater disturbance before they melt than shorter ones (as indicated by the melting temperatures of *n*-alkanes with an even number of carbon atoms[32]). Thus, melting of the non-zwitterionic salts entails progressively larger entropy increases as the chain lengths increase. The zwitterions, in which the cationic and anionic centers cannot diffuse from each other and are limited in their orientations with respect to each other, are able to retain specific intramolecular electrostatic interactions at higher temperatures than their ***m*P*n*X** or ***m*P*n*YX** analogues. Also, the crystalline phases may be more energetic intrinsically as a result of the restrictions imposed on packing near the headgroup by the covalent attachment of the cationic and anionic centers; powder X-ray diffraction measurements indicate less defined lamellar packing in the zwitterions (vide infra). In either case, more disorder among the chains of the zwitterions is necessary for melting to occur, and the incremental decrease in melting temperatures is smaller than the incremental decrease in the enthalpy change as the chains become longer.

Powder X-ray Diffraction (PXRD). All of the salts reported here, except the **1P*n*CO$_2$** zwitterions, show peak progressions in the PXRD diffractograms of their solid phases that are characteristic of lamellar structures; spacing ratios corresponding to 1, 1/2, 1/3, etc.[33] can be found, although some of the higher order reflections are absent in some of diffractograms (Figure 5 and Figure S5 of Supporting Information). The diffractograms demonstrate that different solid morphs for some of salts were obtained from solvent crystallization and melt solidification. However, all of the diffractograms of the liquid-crystalline phases exhibit one narrow low-angle peak ($2\theta < 5°$) and one broad peak near 20° in 2θ (corresponding to 4.4 Å in d). They correspond to the lamellar thickness and intralayer (i.e., interchain) distances, respectively.[34]

The distance between a phosphorus nucleus and the outmost hydrogen atom on a terminal carbon atom of a linearly extended *n*-tetradecyl chain in a single-crystal **1P14CONH$_2$Br** or **1P14CO$_2$HBr** is 19.6 Å. From this value, extended chain lengths for $n = 10$ of 14.5 Å and $n = 18$ of 24.7 Å can be estimated.[35] The lamellar thicknesses d within the liquid-crystalline phases are between one and two times these extended lengths (Table 3). On this basis and given the fact that the molecular directors are orthogonal to the lamellar planes (from POM data; vide ante) the mesophases are assigned to be smectic A_2 (SmA_2).

The dependence of the lamellar thickness d on temperature (and phase) has been investigated by PXRD (Figure 5B and C). Precipitous changes in d occur at temperatures that correlate well with the phase transition temperatures measured in DSC thermograms of the second heating of samples. Within a solid phase, d is almost independent of temperature; solid−solid transitions are accompanied by a detectable change of d. However, the lamellar thicknesses decrease with increasing temperature within a SmA_2 phase as a result of

(32) Briard, A. J.; Bouroukba, M.; Petitjean, D.; Dirand, M. *J. Chem. Eng. Data* **2003**, *48*, 1508–1516.

(33) Stout, G. H.; Jensen, L. H. *X-ray Structure Determination, A Practical Guide*, 2nd ed.; Wiley: New York, 1989; pp 24−28.

(34) Collings, P. J. *Liquid Crystals,* 2nd ed.; Princeton University Press: Princeton, NJ, 2002; pp 74−75.

(35) According to the **1P14CONH$_2$Br** and **1P14CO$_2$HBr** single-crystal data, the length of four linearly extended methylene groups is 5.1 Å. This value was used to estimate the length of incremental decrease or increase in length of extended $n = 10$ or $n = 18$ chains. The influences of temperature and differences in molecular structures (e.g., the nature of anions and the structure of the short chain) were not taken into account in these estimations.

TABLE 2. Enthalpies (ΔH), Entropies (ΔS), and Onset Transition Temperatures (T_o) of K → K, K → SmA_2, and SmA_2 → I Phase Transitions for Salts from DSC Thermograms[a]

		1st heating		1st cooling		2nd heating		
compound	transition	T_o (°C)	ΔH (kJ/mol)	T_o (°C)	ΔH (kJ/mol)	T_o (°C)	ΔH (kJ/mol)	ΔS (J/mol·K)
1P10I	$K_1 \rightarrow K_2$	40.4	1.0	42.5	1.2	38.9	1.1	3.5
	$K_2 \rightarrow I$	60.7	4.0	63.3	3.9	61.5	4.0	12.0
1P10Tf$_2$	$K_1 \rightarrow K_2$	−46.5	−27.9			−47.2	−27.7	
	$K_2 \rightarrow K_3$	−28.9	−8.8			−28.9	−8.5	
	$K_3 \rightarrow I$	−0.5	46.6			−0.2	47.0	
1P10CONH$_2$Br	$K \rightarrow I$	−14.3	2.2	−18.0	2.3	−14.3	2.2	8.8
1P10CO$_2$HBr	$K \rightarrow I$	53.9	2.9	51.4	3.0	53.6	3.0	9.2
2P10OHNO$_3$	$K \rightarrow I$	33.4	56.6	23.7	2.0	29.2	52.1	
2P10OHBF$_4$	$K_1 \rightarrow K_2$	−27.6	−11.6	−39.7	9.7	−25.1	−9.9	
	$K_2 \rightarrow I$	0.8	30.1	−22.7	0.8	0.3	29.6	
1P14I[b]	$K_1 \rightarrow K_2$	37.6	47.1	21.4	30.0	25.8	30.5	102
	$K_2 \rightarrow SmA_2$	62.7	3.0	62.5	2.9	62.4	3.0	8.9
	$SmA_2 \rightarrow I$	112.4	4.0	112.3	4.0	112.3	4.1	10.6
1P14PF$_6$	$K \rightarrow SmA_2$	55.1	55.8	33.9	56.0	47	54.1	176
	$SmA_2 \rightarrow I$	83.0	9.8	82.3	8.7	82.5	9.4	26.4
1P14Tf$_2$	$K \rightarrow I$	46.2	85.1	37.9	82.7	45.8	82.1	262
1P14CONH$_2$Br	$K \rightarrow I$	57.2	98.9	42.4	4.3	43.4	4.2	13.5
1P14CO$_2$HCl	$K_1 \rightarrow K_2$	64.4	62.7	36.6	33.3	59.5	30.6	99.5
	$K_2 \rightarrow I$	99.4	18.5	101.4	18.5	99.2	18.5	49.6
1P14CO$_2$HBr	$K \rightarrow SmA_2$	68.7	92.0	57.1	41.5	69.9	41.5	123
	$SmA_2 \rightarrow I$	88.2	3.8	87.9	3.7	88.3	3.7	10.2
1P14CO$_2$HPF$_6$	$K_1 \rightarrow K_2$	41.1	33.7					
	$K_2 \rightarrow K_3$	54.3	48.9	34.2	51.4	54.7	50.4	160
	$K_3 \rightarrow I$	83.6	9.2	81.9	9.3	83.3	9.1	25.9
2P14OHF	$K \rightarrow I$	30.0	68.0	19.2	31.5	17.3	31.7	108
2P14OHNO$_3$	$K_1 \rightarrow K_2$	34.2	6.9					
	$K_2 \rightarrow I$	38.0	77.4	17.5	46.7	28.0	47.4	159
2P14OHBF$_4$	$K_1 \rightarrow SmA_2$	39.2	85.0	21.9	38.8	29.6	48.6	145
	$SmA_2 \rightarrow I$	60.2	3.1	63.6	3.1	60.3	3.1	9.3
2P14OHClO$_4$	$K_1 \rightarrow K_2$	38.3	9.5	20.4	27.1	37.5	11.3	
	$K_2 \rightarrow I$	45.2	82.4	16.7	52.4	42.6	73.6	
2P14OHTf$_2$	$K \rightarrow I$	29.9	47.8	5.9	56.6	28.1	56.7	195
1P18Tf$_2$	$K \rightarrow I$	66.5	119	55.0	105	66.1	106	315
1P18CONH$_2$Br	$K_1 \rightarrow K_2$			47.3	45.3			
	$K_2 \rightarrow I$	60.6	129	50.8	9.7	49.8	65.0	
1P18CO$_2$HCl	$K_1 \rightarrow K_2$	88.5	58.5	74.8	51.0	89.6	50.7	143
	$K_2 \rightarrow I$	97.8	22.7	97.9	22.4	97.8	22.4	60.4
1P18CO$_2$HBr	$K_1 \rightarrow K_2$	67.5	28.1			67.3	27.5	
	$K_2 \rightarrow I$	83.7	57.3	70.0	86.2	83.2	58.0	
1P18CO$_2$HClO$_4$	$K \rightarrow I$	69.7	120	60.8	105	67.0	103	309
2P18OHF	$K_1 \rightarrow K_2$	50.2	8.3	40.0	8.6	49.0	8.0	26.1
	$K_2 \rightarrow K_3$	57.5	1.5	48.2	16.2	52.7	2.9	
	$K_3 \rightarrow I$	64.4	34.2	60.3	23.4	58.6	33.0	
2P18OHBF$_4$	$K_1 \rightarrow K_2$					49.6	45.1	
	$K_2 \rightarrow I$	60.7	156	53.4	102	60.2	56.8	
2P18OHClO$_4$	$K_1 \rightarrow K_2$					50.4	67.1	
	$K_2 \rightarrow I$	60.9	137	51.0	85.3	58.2	25.2	
2P18OHTf$_2$	$K \rightarrow I$	55.3	87.0	42.3	73.3	53.9	73.3	228
2P6CO$_2$	$K \rightarrow I$	160.8	138	135.3	135	159.1	134	323
2P10CO$_2$	$K \rightarrow I$	145.0	30.2	139.0	30.1	144.1	30.1	72.7
2P14CO$_2$	$K_1 \rightarrow K_2$	65.6	9.8	46.6	6.1	50.8	6.2	19.1
	$K_2 \rightarrow I$	131.4	28.6	127.1	26.4	129.8	26.7	66.2
2P18CO$_2$	$K_1 \rightarrow K_2$			84.9	14.2			
	$K_2 \rightarrow K_3$	86.1	15.1	91.6	3.4	88.8	16.8	
	$K_3 \rightarrow I$	119.7	28.6	116.2	24.5	119.2	24.3	62.6
3P10SO$_3$	$K_1 \rightarrow K_2$	45.2	84.9					
	$K_2 \rightarrow K_3$	80.5	141					
	$K_3 \rightarrow I$	147.6	78.3	140.9	79.0	147.7	79.3	190
3P14SO$_3$	$K_1 \rightarrow K_2$	47.3	5.0					
	$K_2 \rightarrow K_3$	88.1	33.1					
	$K_3 \rightarrow I$	132.8	13.8	136.0	13.4	134.4	12.8	32.1
3P18SO$_3$	$K_1 \rightarrow K_2$			59.0	40.0	57.1	20.8	
	$K_2 \rightarrow K_3$	99.9	41.0			101.3	29.6	
	$K_3 \rightarrow I$	122.9	12.2	125.5	12.3	126.3	12.6	31.2

[a] Averaged onset temperatures from endothermic and exothermic peaks for the same transition from DSC thermograms of first cooling and second heating of the salts. [b] The **1P14I** salt contains a trideutriomethyl group attached to phosphorus.

the greater frequency of *gauche* bends (and less extended chains). For similar reasons, the full-width-at-half-height (fwhh) of the low-angle peaks is larger in the SmA_2 phases than in the solid phases. Even in the isotropic phase, some residual molecular ordering must be retained because a low angle peak, albeit weak and broad, is present at temperatures well above T_C. The lamellar thickness is reduced upon addition of a covalently attached functional group near ionic regions or replacement of a smaller anion with a larger one (Table 3 and Table S7 of Supporting Information), as expected, because both structural changes make the projection of the molecules on their layer planes larger.

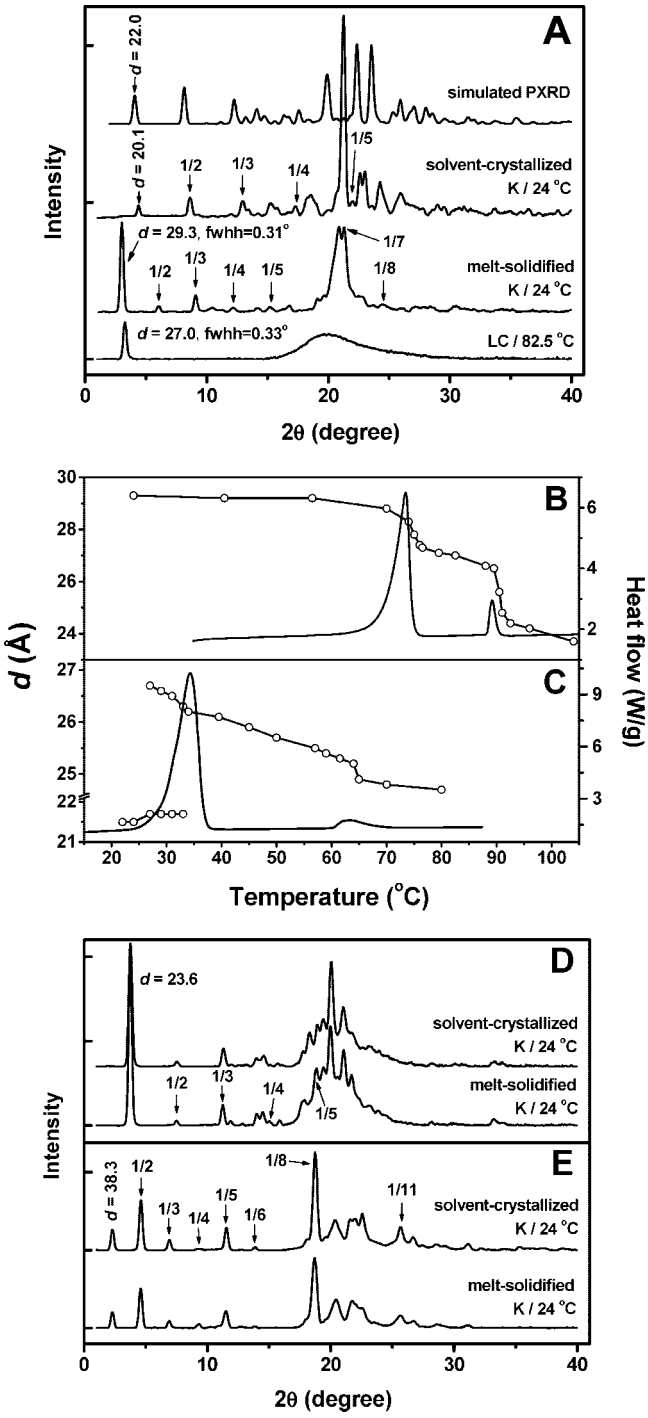

FIGURE 5. X-SEED simulations (from single-crystal diffraction data at −100 °C) of powder X-ray diffractograms and diffractograms from solvent-crystallized, melt-solidified, and liquid-crystalline (LC) phases of **1P14CO$_2$HBr** (A). Superposed heat flows from DSC thermograms (solid lines) and lamellar spacings (*d*, Å) by X-ray diffraction (○) as a function of temperature for (B) **1P14CO$_2$HBr** and (C) **2P14OHBF$_4$**; X-ray diffractograms of the solvent-crystallized and melt-solidified solid phases of (D) **2P10CO$_2$** and (E) **3P10SO$_3$**. Ethyl acetate was used as the solvent to obtain both the single-crystal and powder samples here.

The X-SEED simulation from single-crystal data at −100 °C and XRD patterns from solvent-crystallized powder at room temperature for **1P14CO$_2$HBr** are very similar, but there are notable differences (Figure 5A); similar differences were detected in the single-crystal-derived and powder diffractograms of **1P14CONH$_2$Br** also (Figure S5A of Supporting Information). Because both the single-crystal and powder samples of **1P14CO$_2$HBr** were obtained from solutions of ethyl acetate, the differences may indicate that a solid−solid phase transition occurs at an intermediate temperature. The differences between single-crystal and powder samples of **1P14CONH$_2$Br** may be related to their being obtained by crystallization from different solvents, acetonitrile and ethyl acetate, respectively. None was observed for both powder samples by DSC between 24 °C and the lowest temperature accessible instrumentally, −85 °C. Thus, we attribute the differences and slightly smaller lamellar thickness at room temperature to more interdigitation and *gauche* bending of long alkyl chains that become allowed as the solids are warmed and become less ordered.

The percent extent of chain interdigitation (ECI) between ionic planes is defined here as the length of overlap of the nonpaired, long *n*-alkyl chains of two antiparallel molecules between bilayers, $100(2d_C - d)/d$, where d_C is the extended length of a long *n*-alkyl chain[35] and *d* is the lamellar thickness from X-ray powder diffractograms (Table 3 and Table S7 of Supporting Information). No ECI values within the liquid-crystalline phases were calculated because the long chains there are not "static" or extended.

The slightly larger lamellar thickness of **1P14CONH$_2$Br** in both its solvent-crystallized and melt-solidified solid phases compared with those of the corresponding **1P14CO$_2$HBr** may be understood from the single-crystal structures. The P^+-X^- and H-bonding distances are longer in **1P14CONH$_2$Br** than in **1P14CO$_2$HBr**, suggesting weaker interactions of molecules within the ionic layers of the former. In addition, the *d* values of both salts indicate that the lamellae of their melt-solidified morphs are less interdigitated than those of the solvent-crystallized morphs. The lamellae are maintained in all solid phases of these salts and show a lower ECI in the higher temperature phase of the two solids detected. It appears that adjustments of chain interdigitation and, consequently, of conformations within ionic regions are primarily involved in the solid−solid transitions. Liquid-crystallinity is favored when the solid phases of salts with relatively low ECIs (e.g., **1P14CO$_2$HBr** in Figure 5B) are heated or melting is accompanied by a significant reduction in the ECI (e.g., **2P14OHBF$_4$** in Figure 5C).

The thermal instability of the **1P*n*CO$_2$** zwitterions (vide supra) precluded their investigation in melt-solidified forms. The methanol-crystallized materials do not appear to pack in lamellae on the basis of their powder X-ray diffractograms (Figure S6 of Supporting Information). The anionic center at the end of the 1-carboxymethyl chain probably leads to an alternative packing arrangement that maximizes ionic interactions at the expense of layering; the nature of that packing is not obvious from the information in hand. The precursor **1P*n*CO$_2$HBr** salts *do* pack in layers as do the zwitterions that are homologous to the **1P*n*CO$_2$**, the **2P*n*CO$_2$** with carboxyethyl chains (Figure 6A).

From single-crystal structures, the molecular lengths of **1P14CONH$_2$Br** and **1P14CO$_2$HBr** are 37.3 Å. This value allows values for the homologous $n = 10$ and $n = 18$ salts, 27.1 and 47.5 Å, respectively, to be deduced.[35] The lamellar thicknesses of the **3P*n*SO$_3$** zwitterions are between one and two times their extended molecular lengths. The lamellar packing structure of the **3P*n*SO$_3$** zwitterions, evidenced by X-ray diffractometry, suggests that cations and anions should be alternatively arranged within lamellae.[14a,15,18] We hypothesize

TABLE 3. Comparisons of Lamellar Spacings (d, ±0.1 Å) and Extents of Their Chain Interdigitations (ECI, %; See Text)[a]

compound	T (°C)	phase	d (Å)	ECI (%)	compound	T (°C)	phase	d (Å)	ECI (%)
1P10I	24	K	19.2	47	**1P10CO$_2$HBr**	24	K	20.9	35
2P10OHNO$_3$	24	K	19.8	42	**1P14CONH$_2$Br**	−100	K[b]	21.6	77
2P10OHCl	24	K	22.7	24		24	K[c]	20.8	84
	67	SmA$_2$	20.7			24	K	29.2	31
2P10OHBr	24	K	22.0	28	**1P18CONH$_2$Br**	24	K	46.7	3
	57	SmA$_2$	20.3		**1P18CO$_2$HCl**	24	K$_1$	36.9	31
1P14I	24	K	27.8	37		92	K$_2$	39.8	21
	85	SmA$_2$	26.0		**1P18CO$_2$HBr**	24	K$_1$	36.4	32
1P14PF$_6$	24	K	20.7	85		77.5	K$_2$	36.5	32
	65	SmA$_2$	25.2		**1P18CO$_2$HClO$_4$**	24	K	27.1	79
1P14Tf$_2$	24	K	22.7	68	**2P18OHF**	24	K	48.0	0
1P14CO$_2$HCl	24	K$_1$	29.6	29	**2P18OHCl**	24	K	32.8	47
	81	K$_2$	31.3	22		90.5	SmA$_2$	31.0	
1P14CO$_2$HBr	−100	K[b]	22.0	74	**2P18OHBr**	24	K	34.9	38
	24	K[c]	20.1	90	**2P18OHBF$_4$**	24	K	28.7	68
	24	K	29.3	30	**2P18OHClO$_4$**	24	K	27.2	77
	82.5	SmA$_2$	27.0		**2P18OHTf$_2$**	24	K	26.9	79
1P14CO$_2$HPF$_6$	24	K$_1$	21.1	81	**1P18Tf$_2$**	24	K	27.6	75
	80	K$_2$	26.9	42	**2P6CO$_2$**	24	K	14.6	25
2P14OHF	24	K	33.7	13	**2P10CO$_2$**	24	K	23.7	19
2P14OHNO$_3$	24	K	26.0	47	**2P14CO$_2$**	24	K	40.3/30.8[d]	24[e]
2P14OHCl	24	K	26.5	44	**2P18CO$_2$**	24	K	38.6	25
	82	SmA$_2$	27.1		**3P10SO$_3$**	24	K	38.6	
2P14OHBr	24	K	25.6	49	**3P14SO$_3$**	24	K	52.0	
	79.5	SmA$_2$	26.5		**3P18SO$_3$**	24	K	34.0	
2P14OHBF$_4$	24	K	21.6	77		24	K[c]	63.9	
	50	SmA$_2$	25.7						
2P14OHClO$_4$	24	K	21.6	77					
2P14OHTf$_2$	24	K	22.3	71					

[a] From powder X-ray diffraction data for ***m*P*n*YX**, **1P*n*Tf$_2$**, **1P*n*I** (n = 10, 14), and **1P14PF$_6$** salts, and zwitterionic salts in their SmA$_2$ and (except as noted) melt-solidified (K) phases at different temperatures. Data for **2P*n*OHX** (X = Cl or Br) are from ref 16. [b] Single-crystal solid phase. [c] Solvent-crystallized solid phase. [d] The X-ray diffractogram of melt-solidified **2P14CO$_2$** contains two low-angle peaks (Figure S5C of Supporting Information). [e] The calculated ECI is based on the diffraction corresponding to d = 30.8 Å.

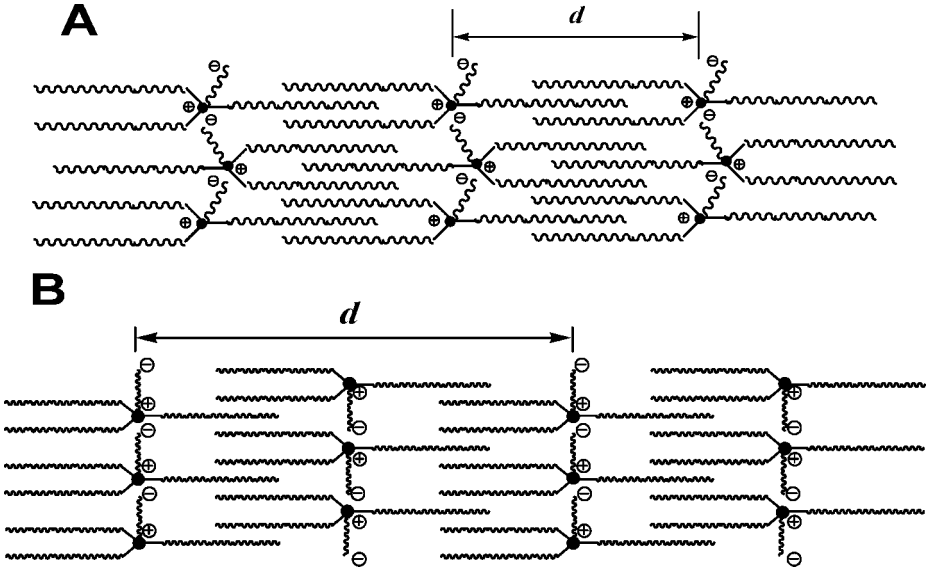

FIGURE 6. Cartoon representation of the proposed bilayer lamellar packing arrangements for phosphonium zwitterions. The chains, especially the shortest chain with the covalent attachment of anions may not extend straightly in packing structures as shown here, and it is only for clarity to indicate an overall direction of the shortest chain.

that their 3-sulfopropyl chains are oriented somewhat within the ionic planes and, therefore, away from the long molecular director formed by three long *n*-alkyl chains. On the basis of these considerations, we propose that the **3P*n*SO$_3$** zwitterions adopt a lamellar packing arrangement similar to that of the **2P*n*CO$_2$**, but with the shortest chains localized at or near ionic planes in some fashion (Figure 6B). The lamellar thickness of melt-solidified **3P18SO$_3$**, much smaller than that of the solvent-crystallized solid, is between one and two times of the length of an extended *n*-octadecyl chain. It suggests that the melt-solidified **3P18SO$_3$** adopts a different bilayer packing structure, like that in Figure 6A, than the one obtained by solvent crystallization. In this regard, note that the first and second heating DSC thermograms for this salt are very different (Figure S7 of Supporting Information).

The lamellar packing structures of the solid phosphonium zwitterions investigated here have some of the attributes that appear necessary to melt into liquid-crystalline phases. However, the lack of freedom of motion afforded the covalently attached carboxylate or sulfonate anionic centers at the end of the short

alkyl chains appears to inhibit liquid crystallinity by making more difficult the maintenance of the ionic planes after the long *n*-alkyl chains melt.

Conclusions

The molecular structures and phase properties of a large number of phosphonium salts with 3 long *n*-alkyl chains have been correlated to determine the factors leading to liquid-crystalline phases. Except for the **1P*n*CO$_2$** zwitterions, the phosphonium salts and zwitterions investigated here appear to pack in bilayer lamellar structures with different degrees of interdigitation in their solid phases. Empirically, some interdigitation appears to be necessary to maintain the long-range phase orientation, which depends on a combination of the length of the three long *n*-alkyl chains, the structure of the short group attached to the positively charged phosphorus atom, and the nature of the anion, as well as other intra- and intermolecular interactions.

Subtle changes in molecular structure can induce large changes in phase properties. Thus, **1P*n*X** salts with small anions do not form liquid-crystalline phases. They have relatively well-defined packing structures because the small anion and methyl group on phosphorus allow strong intra- and intermolecular P^+-X^- ionic interactions within ionic layers of the solid. The **1P*n*X** with larger anions have more disturbed ionic layers. When their *n*-alkyl chains are longer, they are better able to maintain their layered structures upon melting. Alternatively, a hydroxymethylene, carboxy, or amido functional group Y, when attached to the α-methyl of **1P*n*X** salts (including in forms leading to zwitterions), weakens the intramolecular P^+-X^- ionic interactions within the ionic layers and increases the importance of relatively weak intramolecular $X^-\cdots H(Y)$ interactions. However, the additional concurrent increase in disorder within the lamellae of these salts is found to frustrate melting into liquid-crystalline phases.

Another method to induce or augment liquid crystallinity in phosphonium salts has been reported recently.[16,19] In it, one or more equivalents of water or an alcohol are added to a **1P*n*X** salt so that the effective headgroup area is increased. That approach weakens P^+-X^- ionic interactions via solvation of the P^+ and X^- components of the **1P*n*X** salts.

All of the liquid-crystalline phases formed here are assigned to be smectic A_2, and the degree of their chain interdigitation is no higher than that in their solid phases. For different salts with the same length for their three long *n*-alkyl chains, both the lamellar thicknesses and clearing temperatures of the phosphonium salts decrease with increasing size of the anions or short chain on phosphorus. Also, the clearing temperatures *decrease* in salts but *increase* in zwitterions as the lengths of the long *n*-alkyl chains increase. Thus, it is possible to use these criteria to design (or select from among the existing materials reported here) a phosphonium salt whose liquid-crystalline temperature range and structural properties match an application need.

These salts have several characteristics that may make them prefereable for many applications to the more common ionic liquid crystals based on imidazolium or pyridinium salts.[11] These include their saturated organic structures, simplicity of purification, and lack of absorption in the visible and near-UV regions. Future studies will be directed to examining and exploiting those applications.

Experimental Section

Materials. Tri-octadecylphosphine, tri-tetradecylphosphine, tridecylphosphine, and tri-hexylphosphine were gifts from Dr. Allan Robertson, Cytec Industry, Niagara Falls, Ontario, Canada and were used without further purification. Solvents (HPLC grade), bromoacetic acid (99%), 2-bromoacetamide (98%), acrylic acid (99%), 1,3-propanesultone (98%), potassium ethyl xanthane (98%), hydrochloric acid (37%), nitric acid (70%), hydrofluoric acid (48%), perchloric acid (ACS reagent, 60%), tetrafluoroboric acid (50%), hexafluorophosphoric acid (60%), lithium bis(trifluoromethylsulfonyl) imide (97%), and potassium hydroxide (Certified ACS pellets) were used as received.

General Procedure for the Syntheses of Phosphonium Salts and Zwitterions. In a glovebox purged with nitrogen, a trialkylphosphine was transferred to a round-bottom flask containing a stirring bar. Nitrogen was bubbled for ca. 20 min through a chloroform solution of 1.2 molar equiv of bromoacetic acid, 2-bromoacetamide, acrylic acid, or 1,3-propanesultone as a second reactant in a separate flask that was sealed with a septum (except for nitrogen inlet and outlet needles), and then the liquid was added by syringe to the flask with the phosphine. The combined solution was stirred continuously for 1 day at room temperature under nitrogen, reduced on a rotary evaporator to a clear oil, and recrystallized (3×) from hexanes or ethyl acetate. Salts with $n =$ 14 and 18 were filtered at room temperature; solutions of those with $n = 10$ were cooled in a dry ice bath and filtered using a Büchner funnel packed in dry ice.

Tri-*n*-alkylmethylphosphonium bromide salts (**1P*n*Br**, $n = 10$, 14, or 18) and tri-*n*-alkyl-(2-hydroxylethyl)phosphonium bromide (**2P*n*OHBr**) were available from earlier studies.[16] Syntheses of other phosphonium salts started with these bromides. A mixture of a phosphonium bromide and 1.2 molar equiv of potassium ethyl xanthate in chloroform was stirred for 2−3 days at room temperature and filtered. A concentrated acid containing the anion of choice was added to the yellow filtrate, whose volume was adjusted to form a ca. 0.5 M chloroform solution of phosphonium ethyl xanthate. The mixture was stirred for an additional day, initially in an ice-bath that was allowed to melt slowly to room temperature. The organic layer was washed with deionized water (2 × 20 mL), concentrated to an oil on a rotary evaporator, recrystallized (3×) from hexanes or ethyl acetate, and filtered. Specific quantities employed and physical and spectral characterization data for each of the salts are included in the Supporting Information file.

Acknowledgment. We are grateful to the U.S. National Science Foundation for financial support and to Dr. Al Robertson of Cytec for supplying the trialkylphosphines used in this research.

Supporting Information Available: Characterization data for ***m*P*n*YX**, ***m*P*n*Y**, and some **1P*n*X** salts; ^{1}H NMR spectra for all synthesized salts; thermal gravitational analyses for **1P*n*CO$_2$HBr** and **2P*n*CO$_2$**; molecular conformations and H-bonding interactions of **1P14CONH$_2$Br** and **1P14CO$_2$HBr** from their single-crystal structures; transition temperatures determined by optical microscopy; DSC thermograms for **1P*n*X** and **3P18SO$_3$**; powder X-ray diffractograms for zwitterions and **1P10I**; lamellar thicknesses for **1P*n*X** at selected temperatures of solid and liquid-crystalline phases. This material is available free of charge via the Internet at http://pubs.acs.org.

JO802605K